Magnetic resonances in metallic double split rings: Lower frequency limit and bianisotropy

Lei Zhou[a)]
Surface Physics Laboratory, Fudan University, Shanghai 200433, People's Republic of China

S. T. Chui
Bartol Research Institute, University of Delaware, Newark, Delaware 19716

(Received 14 September 2006; accepted 12 December 2006; published online 22 January 2007)

The authors employ a rigorous theory to study the electromagnetic resonances in double split rings of circular cross sections. The inter-ring interactions split each single-ring mode to two modes with different symmetries, and the bianisotropy of each mode is suppressed as two rings approach. They obtain analytical expressions to estimate the frequency of the fundamental (magnetic) mode, which facilitate the design of structures with the lowest possible resonance frequencies. Numerical calculations based on the present theory are supported by finite-difference-time-domain simulations on realistic structures and experimental data published previously. © *2007 American Institute of Physics*. [DOI: 10.1063/1.2431776]

As the building blocks of recently discovered left-handed metamaterials (LHM),[1] metallic ring systems have attracted considerable attention recently.[2–11] Previous theoretical understandings on such systems were achieved mainly through analytical methods[2–7] or numerical simulations.[8–11] The former[2–7] oversimplified the complicated inductive/capacitive effects. Although the full-wave simulations[8–11] provided highly reliable results, it was not easy to extract the polarizabilities of a building block directly from the obtained results.[8] Recently, we established a rigorous approach for metallic ring systems and applied it to study the electromagnetic (EM) eigenmodes of a single split ring resonator (SRR) of circular cross section.[12]

To realize a LHM sample with a good quality, one requires the building block to be as *subwavelength* as possible and its *bianisotropy* as small as possible. In this letter, we extend our theory[12] to study the EM resonances in a double-ring SRR, with attention mainly focused on the above two properties. We found that the ring-ring interactions split each single-ring mode to two modes with different symmetries (see Ref. 7 for a similar conclusion), and the bianisotropy of each mode decreases significantly as two rings approach. We derived analytical formulas to estimate the resonance frequency of the fundamental (magnetic) mode and showed how to lower this frequency.[6,7] In contrast to previously derived analytic formulas,[6,7] our formulas are explicit functions of geometrical parameters. The validities of our formulas are supported not only by our own finite-difference-time-domain (FDTD) simulations but also by experimental data published previously.[13,14]

We consider N concentric metallic rings placed on the xy plane, each having a radius R_i and a renormalized resistivity function $\tilde{\rho}_i(\phi)$.[12] We assume that the metallic wire forming each ring has a circular cross section with a radius a_i. Driven by an external field $\mathbf{E}_{\text{ext}}(\mathbf{r})$, a current $\mathbf{j}_i(\mathbf{r}) = \mathbf{e}_\phi I_i(\phi)\sin\theta\delta(\cos\theta)\delta(r-R_i)/R_i$ is induced in the ith ring.[15] Following the method described in Ref. 12, we obtain a matrix equation, $\Sigma_{m'j} H^{\{i,m\}}_{\{j,m'\}} I_{\{j,m'\}} = E^{\{i,m\}}_{\text{ext}}$, to determine $\mathbf{j}_i$ in terms of $\mathbf{E}_{\text{ext}}$. The matrix elements are given by

$$H^{\{i,m\}}_{\{j,m'\}} = \tilde{\rho}_i(m-m')\delta_{ij} + i\omega L^{i,j}_m (1-(\Omega^{ij}_m/\omega)^2)\delta_{mm'}, \qquad (1)$$

in which $L^{i,j}_m$ are the inductance elements and Ω^{ij}_m the bare resonance frequencies, which can be obtained following the method described in Ref. 12. $\tilde{\rho}_i(m)$, $I_{\{i,m\}}$, and $E^{\{i,m\}}_{\text{ext}}$ are the Fourier components of $\tilde{\rho}_i(\phi)$, $I_i(\phi)$, and $E^i_{\text{ext}}(\phi) = \mathbf{E}_{\text{ext}}(\mathbf{r} = R_i\mathbf{e}_r)\cdot\mathbf{e}_\phi$, correspondingly, and $c_0 = 1/\sqrt{\varepsilon_0\mu_0}$ is the speed of light. Solving the matrix to obtain a series of eigenvalues $\lambda_l(\omega)$, we determine the resonance frequencies by the condition that $|\min[\lambda_l(\omega)]|$ exhibits a minimum.[12] The dipole moments induced by the external field, P_x, P_y, and M_z, can also be calculated.[12]

We study a double-ring SRR,[2] with $R_1 = R$, $R_2 = R-d$, and $a_1 = a_2 = a \ll R$. A gap of a width Δ is opened at $\phi = 0$ for the outer ring and at $\phi = \pi$ for the inner ring. We set the resistivity $\tilde{\rho} = 0$ for the metal and $\tilde{\rho} = \tilde{\rho}_0 \to \infty$ for the air gap. The infinite resistivity stops the current flow through the gap, leading to charge accumulations on the rings. This is the origin of the gap capacitance effect, which is treated rigorously here. For a specific example, we solved the matrix[16] and show in Fig. 1(a) the calculated $\min[|\lambda_l|]$ as a function of ω/ω_0, with $\omega_0 = c_0/R$. Compared with the spectra of a single-ring SRR, we find that each single-ring mode has split into a pair of modes in the double-ring case through mutual inductance/capacitance effects. Each mode pair involves a similar set of Fourier components like its corresponding single-ring mode.[12] We depict in Figs. 1(b) and 1(c) the eigenvectors for the first two modes, which involve mainly the $m = 0, \pm 1$ components, similar to the lowest single-ring mode.[12] Figure 2 shows the dipole moments of the structure induced by different external plane waves, whose $\mathbf{E}$ field and wave vector $\mathbf{k}$ directions are specified in the legend. Similar to the single-ring case,[12] we find that the odd-numbered modes $(\omega^L_1, \omega^H_1, \omega^L_3, \omega^H_3, \ldots)$ carry both electric (P_y) and magnetic (M_z) polarizations, while the even-numbered ones $(\omega^L_2, \omega^H_2, \omega^L_4, \omega^H_4, \ldots)$ carry only electric (P_x) polarizations.

The inter-ring interactions combine components of different rings with a certain relative phase to form a double-

a)Electronic mail: phzhou@fudan.edu.cn

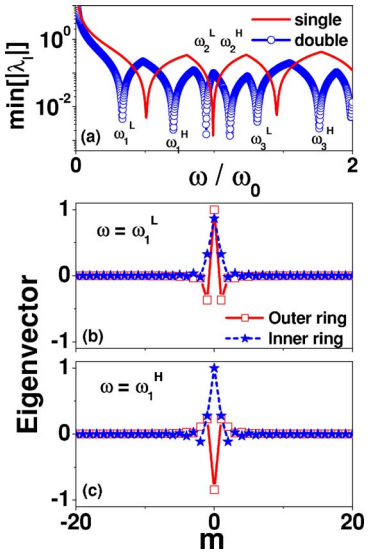

FIG. 1. (Color online) (a) min[$|\lambda_l|$] (in arbitrary units) as the functions of ω/ω_0 calculated for a double-ring SRR (symbols) with $R=4$ mm, $d=0.4$ mm, $a=0.1/\sqrt{\pi}$ mm, and $\Delta=\pi/90$ and a single-ring SRR (lines) with $R=3.8$ mm, $a=0.1/\sqrt{\pi}$ mm, and $\Delta=\pi/90$. Eigenvector component $Q_l^{i,m}$ as functions of m for the outer ring ($i=1$, open squares) and the inner ring ($i=2$, solid stars) for the resonance mode at ω_1^L (b) and at ω_1^H (c).

ring eigenmode.[7] As shown in Figs. 1(b) and 1(c), while the $m=0$ components are in phase for the ω_1^L state and out of phase for the ω_1^H state, the $m=\pm1$ components just behave *oppositely*. Since the $m=0$ ($m=\pm1$) terms contribute to the M_z (P_y) moments, we expect that the magnetic (electric) polarizations must be highly diminished in the ω_1^H (ω_1^L) mode. Figure 2 verifies this argument. Other modes exhibit similar behaviors dictated by their eigenvector properties.

We performed FDTD simulations[17] on realistic SRR structures. The calculated transmission spectra of SRR arrays[18] were shown in Figs. 3(a)–3(d), with the same input EM waves as in Figs. 2(a)–2(d). Comparing Figs. 3(a) and 3(b) with Figs. 2(a) and 2(b), we get a one-by-one correspondence between the transmission dips in Fig. 3 and the moment peaks in Fig. 2, and then we can label the mode indices

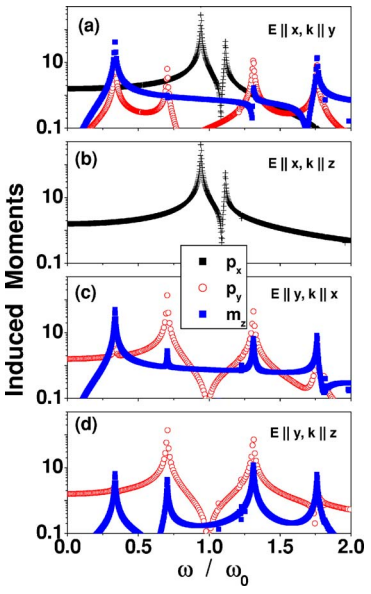

FIG. 2. (Color online) Dipole moments (in arbitrary units) of the double-ring SRR (same as Fig. 1) induced by external plane waves with **E** and **k** directions specified in the legend.

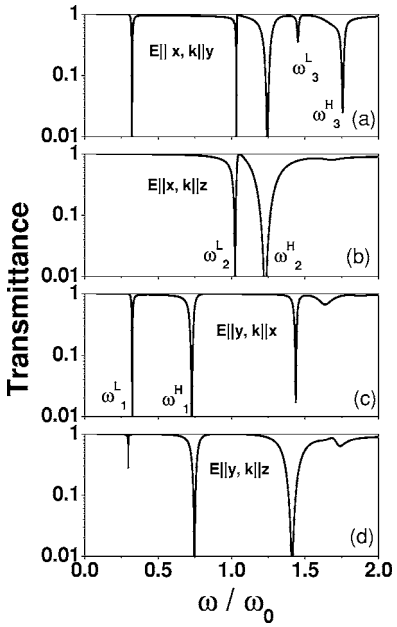

FIG. 3. FDTD simulated transmission spectra of double-ring SRR arrays under plane wave inputs with **E** and **k** directions specified in the legend.

for those dips in Fig. 3. We find that the mode ω_1^H is undetectable in Fig. 3(a), and the mode ω_1^L is very weak in Fig. 3(d), caused by the polarization diminishment effects. In the geometry of Fig. 3(a), the input EM wave is blocked essentially by the P_x or M_z polarizations. The strongly suppressed M_z polarization of the ω_1^H mode is responsible for the missing transmission dip here. The same argument applies to the suppressed transmission dip for the ω_1^L mode in Fig. 3(d).

With the dipole moments shown in Fig. 2, we have derived all elements of the electric/magnetic polarizabilities of the structure, following the definitions in Refs. 4 and 5. We show in Figs. 4(a) and 4(b) the calculated values of electric polarizability (α_{yy}^{ee}) and bianisotropic polarizability (α_{yz}^{em}),[4] respectively, for double-ring SRR's with different values of d. Clearly, both α_{yy}^{ee} and α_{yz}^{em} are significantly suppressed as d decreases.

The magnetic resonance frequency ω_1^L is drastically lowered compared to the single-ring mode (denoted by ω_1). Solid symbols in Fig. 5(a) are the calculated relative frequency shift, i.e., $\delta\omega/\omega_1=(\omega_1^L-\omega_1)/\omega_1$, as functions of d for

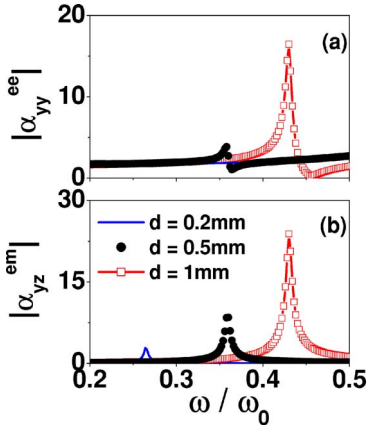

FIG. 4. (Color online) Amplitudes of (a) electric polarizability $|\alpha_{yy}^{ee}|$ and (b) bianisotropic polarizability $|\alpha_{yz}^{em}|$ as functions of ω/ω_0, for double-ring SRR's with $R=4$ mm, $a=0.1/\sqrt{\pi}$ mm, and different values of d specified in the legend.

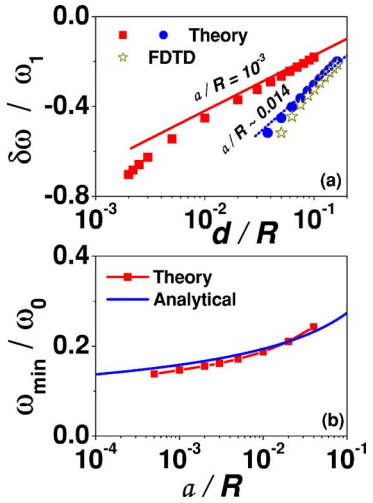

FIG. 5. (Color online) (a) $\delta\omega/\omega_1$ as functions of d/R for two sets of double-ring systems with different values of a/R, calculated by the present theory (solid symbols), FDTD simulations (open symbols), and Eq. (3) (lines). (b) The limiting resonance frequency of a double-ring SRR as functions of a/R, calculated by the complete theory and the analytical formula.

two sets of samples. As expected, $\delta\omega/\omega_1$ becomes larger as d decreases. FDTD simulations are performed on a series of samples, and the results are depicted in Fig. 5(a) as open stars. Excellent agreement is found between the FDTD and theoretical calculations. We derive an approximate analytical expression for $\delta\omega/\omega_1$. As Figs. 1(b) and 1(c) indicate that the ω_1^L and ω_1^H modes mainly involve the $m=0,\pm1$ components, we retain only those terms in the H matrix. When d is small enough, it is safe to set $\Omega_m^{11}\approx\Omega_m^{22}=\Omega_m$, $L_m^{11}\approx L_m^{22}=L_m$. The 6×6 H matrix is diagonalized to yield

$$\omega_1^{\pm}=\sqrt{(L_1\Omega_1^2\pm\tilde{L}_1\tilde{\Omega}_1^2)/(2L_0+L_1\mp(2\tilde{L}_0-\tilde{L}_1))}, \tag{2}$$

where $\tilde{\Omega}_m=\Omega_m^{12}=\Omega_m^{21}$, $\tilde{L}_m=L_m^{12}=L_m^{21}$. The magnetic resonance frequency is $\omega_1^L=\omega_1^-$. In the limit of $R>d\gg a$, we obtain a formula,

$$\omega_1^L=\omega_1[1-2\ln(2d/R)/(3\ln(2a/R))], \tag{3}$$

to determine the resonance frequency in *explicit* terms of SRR parameters (a,d,R, etc.). The physics is that $\delta\omega/\omega_1$ is dictated by a competition between the mutual interaction ($\propto\ln(2d/R)$) and the self-interaction ($\propto\ln(2a/R)$).[12] Lines in Fig. 5(a) are results calculated with such a formula, which agree well with both theoretical and FDTD results, particularly when $d\gg a$.

Equation (2) indicates that ω_1^L is significantly lowered when $d\to a$. For a system with fixed R and a, the minimum value of d is $2a$. Put $d=2a$ into Eq. (2), we get

$$\omega_{\rm lim}\xrightarrow{d\to2a}\omega_0\sqrt{\ln(1/2)/[4\ln(a/R)]}, \tag{4}$$

to estimate the minimum resonance frequency of such a structure. As $a/R\to0$, this frequency approaches zero![2–7] Figure 5(b) shows that $\omega_{\rm lim}$ calculated based on the complete theory can indeed be well described by formula (4).

Our formulas can also be applied (approximately) to SRR's with other cross sections. For the SRR's with rectangular cross sections studied experimentally in Ref. 13, adopting their definitions (i.e., set $R=r-w/2$, $a=w/2$, and $d=t+w$),[13] and taking the experimental data $\omega_1=2\pi\cdot4.58$ GHz,[13] we get

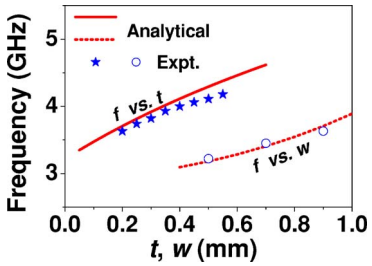

FIG. 6. (Color online) SRR resonance frequency f (measured in GHz) as a function of t (setting $w=0.9$ mm, solid line) and w (setting $t=0.2$ mm, dotted line), calculated by our analytical formula. Symbols are experimental data taken from Figs. 7 and 8 of Ref. 13.

$$f=4.58[1-2\ln(2(t+w)/(r-w/2))/[3\ln(w/(r-w/2))]], \tag{5}$$

to estimate the resonance frequencies of SRR's measured in Ref. 13. Figure 6 shows that the experimental data[13] are reasonably described by our Eq. (5). For the SRR's studied experimentally in Ref. 14, a naive application of our theory [set $R=10.5$ mm, $a=0.5$ mm, and $d=3.4$ mm (Ref. 14)] predicts a relative frequency shift $\delta\omega/\omega_1\sim12.3\%$, smaller than the experimental value of $\sim17.2\%$.[14] However, much better agreement can be obtained if we adjust the *effective radius* of the metal wire to reflect the fact that the SRR's studied in Ref. 14 do not have circular cross sections.

C. T. Chan is thanked for discussions. This work was supported by the NBRPC (No. 2004CB719800), NSFC (No. 10504003), Shanghai Science and Technology Committee, FYTEF, and PCSIRT. S.T.C. was partly supported by the DOE.

[1] V. C. Veselago, Sov. Phys. Usp. **10**, 509 (1968); R. A. Shelby, D. R. Smith, and S. Schultz, Science **292**, 77 (2001).
[2] J. B. Pendry, A. J. Holden, D. J. Robbins, and W. J. Stewart, IEEE Trans. Microwave Theory Tech. **47**, 2075 (1999).
[3] J. Zhou, Th. Koschny, M. Kafesaki, E. N. Economou, J. B. Pendry, and C. M. Soukoulis, Phys. Rev. Lett. **95**, 223902 (2005).
[4] R. Marques, F. Medina, and R. Raffi-El-Idrissi, Phys. Rev. B **65**, 144440 (2002).
[5] R. Marques, F. Mesa, J. Martel, and F. Medina, IEEE Trans. Antennas Propag. **51**, 2572 (2003).
[6] M. Shamonin, E. Shamonina, V. Kalinin, and L. Solymar, J. Appl. Phys. **95**, 3778 (2004); M. Shamonin, E. Shamonina, V. Kalinin, and L. Solymar, Microwave Opt. Technol. Lett. **44**, 133 (2005).
[7] B. Sauviac, C. R. Simovski, and S. A. Tretyakov, Electromagnetics **24**, 317 (2004). N. Lagarkov, V. N. Semenenko, V. A. Chistyaev, D. E. Ryabov, S. A. Tretyakov, and C. R. Simovski, *ibid.* **17**, 213 (1997).
[8] D. R. Smith, S. Schultz, P. Markos, and C. M. Soukoulis, Phys. Rev. B **65**, 195104 (2002).
[9] N. Katsarakis, T. Koschny, M. Kafesaki, E. N. Economou, and C. M. Soukoulis, Appl. Phys. Lett. **84**, 2943 (2004).
[10] P. Markos and C. M. Soukoulis, Phys. Rev. E **65**, 036622 (2002).
[11] Bogdan-Ioan Popa and S. A. Cummer, Phys. Rev. B **72**, 165102 (2005).
[12] L. Zhou and S. T. Chui, Phys. Rev. B **74**, 035419 (2006).
[13] K. Aydin, I. Bulu, K. Guven, M. Kafesaki, C. M. Soukoulis, and E. Ozbay, New J. Phys. **7**, 168 (2005).
[14] A. Radkovskaya, M. Shamonin, C. J. Stevens, G. Faulkner, D. J. Edwards, E. Shamonina, and L. Solymar, Microwave Opt. Technol. Lett. **46**, 473 (2005).
[15] As discussed in Ref. 12, this assumption is valid for a perfect metal with a zero skin depth and for the thin-wire limit (i.e., $a\ll R$).
[16] In all our numerical calculations, we set a cutoff $M_{\rm max}=40$ for the index m and a large air-gap resistivity $\tilde{\rho}_0=10^6\,\mu_0\omega_0$.
[17] K. S. Yee, IEEE Trans. Antennas Propag. **14**, 302 (1966).
[18] CONCERTO 4.0, Vector Fields Limited, England, 2005. Refer to Ref. 12 for computational details.